PROCEEDINGS OF SCIENCE

Precession Polarimetry at JLab, 6 GeV

G.B. Franklin*
Carnegie Mellon University
E-mail: gbfranklin@cmu.edu

The JLab Hall A Compton Polarimeter is used to measure the polarization of the electron beam as it enters the experimental hall. When the polarimeter is in use, the electron beam passes through a Fabry-Perot resonant cavity excited by a laser, allowing the electrons to scatter off the photons. The Compton scattering rate can be measured by detecting the scattered electrons in a silicon microstrip detector or by detecting the back-scattered photons in a calorimeter consisting of a single 6 cm diameter by 15 cm long Ce-doped Gd2SiO5 (GSO) cylindrical crystal. Recent polarimetry measurements have obtained 1% precision using only the photon calorimeter. This talk will start with a review of the features of Compton scattering as they pertain to the polarimeter's statistical and systematic errors. Properties of GSO crystal will be discussed along with benchmark comparisons between GEANT4-based simulations and actual measurements. Features of the custom flash-ADC used to provide deadtime-free integrated photon calorimeter data, along with calorimeter-triggered pulse data, will be reviewed. Contributions to the systematic errors will be discussed.

XVth International Workshop on Polarized Sources, Targets, and Polarimetry,
September 9-13, 2013
Charlottesville, Virginia, USA

*Speaker.

PoS(PSTP 2013)034

1. Compton Scattering as a Polarimetry Tool

1.1 General Considerations

Compton scattering, the scattering of electrons off photons, provides a useful tool for polarimetry because the cross section depends on the relative orientation of the photon and electron spins. Furthermore, this cross section can be calculated from first principles by computing the two leading-order Feynman diagrams shown in Fig. 1. It is also relatively easy to control the spin of the initial-state photons.

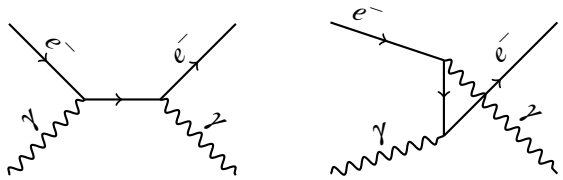

Figure 1: Lowest Order Compton Scattering Diagrams.

In practice, use of the Hall A Compton Polarimeter, shown in Fig. 2, involves energizing a chicane of dipoles to direct the beam through a resonant Fabry-Perot cavity then back to its original trajectory just before it enters Hall A. The Fabry-Perot cavity intensifies the 700 mW laser source to 800 W. Only about 1 in 10^9 electrons actually interacts with the photons, so the measurement is non-destructive. The scattered photons can be detected in a calorimeter located at zero degrees or the scattered electrons that lose energy but are virtually at zero degrees can be detected in a microstrip detector after they are dispersed by the 3^{rd} dipole.

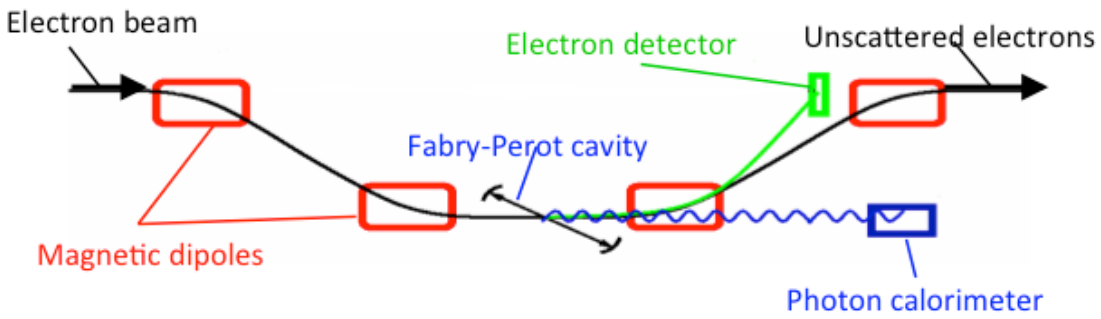

Figure 2: Schematic of Hall A Compton Polarimeter.

The unpolarized Compton scattering cross section was calculated in 1929 and is known as the Klein-Nishina Formula. The scattered photon energies range from a well-defined maximum, known as the Compton edge, down to zero. The Compton edge increases as the square of the electron energy, E, and linearly with the initial photon energy $E_{initial}$; $E_{max} = 4\frac{E^2 E_{initial}}{m_e^2 c^4} a$ where the kinematic factor $a \equiv 1/(1+\frac{4E_{initial}E}{m^2c^4})$ is nearly constant. It is customary to introduce the *normalized photon energy*, ρ, defined as the photon energy divided by the maximum photon energy so that ρ varies from 0 to 1. Figure 3(left) shows the Compton cross section plotted as a function of the

normalized photon energy, ρ. This calculation assumed a 3.48 GeV incident beam and a Fabry-Perot cavity excited by a 1064 nm laser. For these kinematics, the Compton edge ($\rho = 1$) is at $\approx$ 200 MeV.

The spin-dependence of the Compton scattering cross section allows Compton scattering to be used for polarimetry. The longitudinal spin-dependent asymmetry, A_l, is calculated from the spin parallel cross section $\sigma^{\uparrow\uparrow}$ and spin antiparallel cross section $\sigma^{\uparrow\downarrow}$. It can be written in terms of the kinematic factor a, the classical electron radius r_0, and the normalized photon energy ρ:

$$A_l(\rho) \equiv \frac{\sigma^{\uparrow\uparrow} - \sigma^{\uparrow\downarrow}}{\sigma^{\uparrow\uparrow} + \sigma^{\uparrow\downarrow}} = \frac{2\pi r_0^2}{d\sigma/d\rho} a(1-\rho(1+a)) \left[1 - \frac{1}{(1-\rho(1-a))^2}\right].$$

This asymmetry serves as the analyzing power of a polarimeter based on Compton scattering. Figure 3(right) shows A_l for several different incident beam energies and two photon energies. The analyzing power varies approximately linearly with the incident electron beam energy and with the incident photon energy. For example, the analyzing power for scattering 8 GeV electrons off 532 nm photons reaches 20% near the maximum photon energy, $\rho \approx 1$, but it is a strong function of the scattered photon energy and even changes its sign at low scattered photon energy.

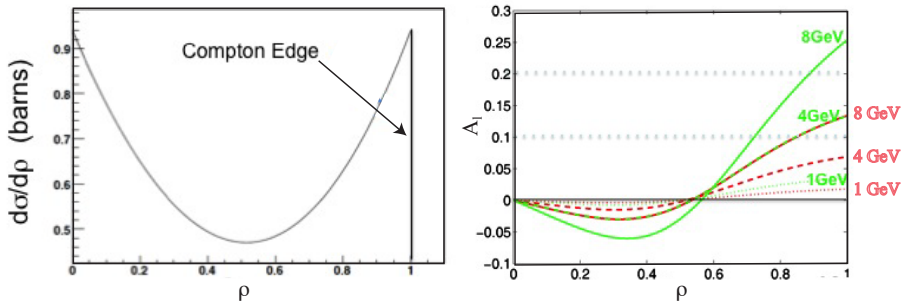

Figure 3: Left: The unpolarized Compton cross section as a function of the normalized scattered-photon energy, ρ (see text). **Right:** The analyzing power as a function of ρ for incident electron beam energies of 1 GeV, 4 GeV, and 8 GeV. The dashed-red curves are calculated for a photon wavelength of λ =1064 nm (1.165 eV) and the solid-green curves correspond to λ =532 nm (2.330 eV).

1.2 Complications

The outgoing photon and electron distributions are extremely forward peaked because the Compton events involve GeV incident electrons scattering off eV photons. This forward peaking is advantageous, in that a photon detector at zero degrees is effectively a 4π detector. But this also creates difficulties because it is not practical to pick off a single scattering-angle and the detection of the scattered photons therefore involves a range of photon energies. The strong energy-dependence of the Compton analyzing power and the range of detected photon energies combine to create a major challenge to minimizing systematic errors. If, for example, a discriminator is used to count events above a fixed threshold, the experiment's effective analyzing power will be a strong function of the discriminator's threshold setting and the resolution function of the detector system.

If an experiment running a 1 GeV beam is followed by an experiment running a 5 GeV beam the Compton edge will increase from roughly 20 MeV to 500 MeV. This large dynamic range

of photon energies makes it difficult to optimize the polarimeter instrumentation. For low energy running, the low Compton-edge energy corresponds to a small energy loss to the scattered electrons and, in this situation, detecting the scattering electrons with a microstrip detector can be difficult because they are not well separated from the beam halo. The detection of the scattered electrons becomes easier at higher beam energies.

Figure 3(right) also shows that obtaining a polarimetry measurement accurate to 1% is particularly difficult at low beam energies since the maximum analyzing power drops to ≈1% for a 1 GeV beam scattering off 1064 nm photons even near the Compton Edge. The analyzing power can be increased by using higher-energy photons. One of the recent Hall A Compton Polarimeter upgrades included the successful installation of frequency-doubling optics that effectively doubles the analyzing power as shown by the green lines.

While the strong energy-dependence of the analyzing power creates some experiment challenges, there is essentially no theoretical challenge. Denner and Dittmaier[1] calculated the slew of next order diagrams and find the higher order terms contribute a 0.3% correction to the analyzing power. This correction can be put into the analyzing power calculations and any terms of yet higher order can be neglected.

2. JLab Hall A Compton Polarimeter

2.1 GSO Calorimeter

The JLab Hall A Compton polarimeter setup, shown in Fig. 2, includes a photon calorimeter located at zero degrees downstream of the Compton interaction point, to measure the scattered photons, and a microstrip detector, to measure the scattered electrons. Either detector can be used to measure the asymmetry and produce a polarization measurement. Additional diagnostic information comes from analyzing the coincident data. Recent Hall A polarimetry work has concentrated on the photon calorimeter and this will be the focus of the remaining discussion. For the photon detector, obtaining a precision measurement requires avoiding threshold-dependent effects and depends on knowledge of the calorimeter's resolution function due to the energy dependence of the analyzing power.

During the upgrade to the Hall A polarimeter, we replaced a multi-element lead-tungstate ($PbWO_4$) calorimeter with a single crystal of Cerium-doped Gd_2SiO_5 crystal (GSO) manufactured by Hitachi Chemical, a cylinder 15 cm long and 6 cm diameter[2][3]. The properties of GSO make it well-suited to this application. It produces two orders of magnitude more light than lead-tungstate and, with a decay time of ≈80 ns, it is nearly as fast. It has a density of 6.7 gm/cm^3, which is only slightly smaller than $PbWO_4$'s density of 8.3 gm/cm^3.

2.2 Integrating DAQ

To avoid systematic errors associated with threshold and dead-time effects, we used a customized Struck 3320 flash ADC to integrate the PMT signal for our primary data analysis.[4][5] For each positive or negative helicity period, the FADC produces a single word which corresponds to the detector signal integrated over a single-helicity period. In the idealized case of a perfectly linear detector-response, this integrated signal can be written in terms of the Compton cross section, $d\sigma/dE$, the longitudinal asymmetry $A_l(E)$, the beam polarization for positive and negative

helicity beam, $P_e^{\pm}$, and the photon polarization, P_γ. Defining the detector efficiency as $\varepsilon(E)$, the energy-summed signal for the positive- and negative -helicity beam periods of luminosity L and time T can be written as

$$E^{\pm} = LT \int_0^{E_{max}} dE\ \varepsilon(E) E \frac{d\sigma}{dE}(E)(1 \pm |P_e^{\pm}| P_\gamma A_l(E)).$$

The measured experimental asymmetry is computed using the energy-summed signals from the positive and negative helicity bins

$$A_{Exp} = \frac{E^+ - E^-}{E^+ + E^-}.$$

In practice, the detector response is not perfectly linear and exhibits event-by-event fluctuations. We define the average detector signal to be $s(E)$ for photons of energy E. The integrated signal can then be written as

$$S^{\pm} = LT \int_0^{E_{max}} dE\ s(E) \frac{d\sigma}{dE}(E)(1 \pm |P_e^{\pm}| P_\gamma A_l(E)).$$

For the JLab experiments utilizing the polarimeter, it is sufficient to determine the helicity-averaged beam polarization, $P_e = (|P_e^+| + |P_e^-|)/2$. In this case, the signal-weighted asymmetry can be written as

$$A_{Exp} \equiv \frac{S^+ - S^-}{S^+ + S^-} = P_e P_\gamma A_{lS}$$

where the calculated signal-weighted analyzing power is

$$A_{lS} \equiv \frac{\int_0^{E_{max}} dE\ s(E) A_l(E) \frac{d\sigma}{dE}(E)}{\int_0^{E_{max}} dE\ s(E) \frac{d\sigma}{dE}(E)}.$$

Accurate calculations of the analyzing power, A_{lS}, are required to determine the beam polarization, P_e, from the measured asymmetry, A_{Exp}. This, in turn, requires careful modeling of the detector to determine $s(E)$.

3. Performance

The typical Compton polarimeter counting rate is of order 100 kHz. At this rate, a statistical accuracy of 1% or better can be reached in a few hours of running. Thus the precision of the polarization measurement for an experiment that runs for many weeks is determined by systematic uncertainties, specifically uncertainties in the determination of the analyzing power, A_{lS}, and the polarization of the cavity photons, P_γ. The measurement of P_γ will be discussed in the next talk. This section will discuss the determination of the photon calorimeter's response function, $s(E)$, since it is required to calculate the signal-weighted analyzing power, A_{lS}.

The electromagnetic showers created by the Compton-scattered photons in the GSO crystal are simulated using GEANT4. To obtain an accurate simulation of the detector response, it is necessary to track the optical photons generated during the ionization process since the fraction of photons that reach the PMT photocathode varies with the geometry of the electromagnetic shower.

Figure 4(left) shows the calculated number of photons reaching the PMT divided by the incident photon energy plotted as a function of the incident photon energy. This quantity decreases slowly with photon energy at low energies but is nearly constant for photons above 50 MeV.

The GSO is read out by a 2 inch diameter PMT whose output is integrated by the FADC. The linearity of the combined PMT/FADC readout is monitored with a two-LED pulser system.[6] The pulser system is used initially to select a PMT/customized tube-base combination that provides an approximately linear signal response over the range of energies corresponding to Compton-scattered photons. Figure 4(right) shows the pulser data for two example PMT-tube base combinations. The pulser system is also used in-situ during the running of the experiment to continuously monitor the linearity and gain shifts. The measured non-linearities are fed into the Monte Carlo simulation and are included in the calculation of the response function $s(E)$.

The non-linearities determined by the GSO simulation and the LED pulser system affect the calculation of the signal-summed analyzing power, A_{ls}, at the level of a few percent. Auxiliary measurements were taken to assure that the simulation of the calorimeter response is accurate. As an example, the calorimeter was taken to Duke University's HIGS photon beam and data were taken with photon energies of 20, 22, 25, 30, and 40 MeV. The known photon-beam characteristics of the HIGS facility were folded into the simulation and the resulting resolution functions were found to be in excellent agreement with the measured photon spectra.[3]

Once the calorimeter was installed in the JLab polarimeter, it is was necessary to avoid misalignments of the collimator and calorimeter that could distort the Compton spectrum and create discrepancies between the simulated data and the actual data. For this purpose, a pair of 1 mm wide tungsten/scintillator beam scanners were affixed to the front face of the GSO and used to monitor the Compton count rate as the entire calorimeter was moved both vertically and horizontally. This procedure provided the means to center the GSO crystal on the Compton beam.

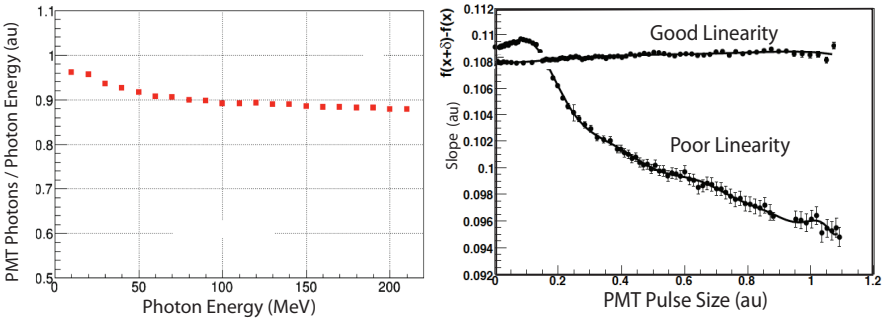

Figure 4: Left:) GEANT4 simulation of photons reaching PMT vs initial photon energy. **Right:** Linearity measurements of two PMT/base combinations using the 2-LED pulser system.

In addition to providing a data word representing the integrated Compton calorimeter signal for each helicity bin, the DAQ data-stream includes data words representing the PMT signal from individual Compton events. Although these sampled events represent only a small fraction of the Compton events, they provide an additional means of verifying the accuracy of the calculated response function $s(E)$. Figure 5(a) illustrates the agreement between the energy spectrum obtained from the event-by-event Compton calorimeter data (shown as individual data points) and the pre-

dictions from the Monte Carlo simulation (solid line). The horizontal axis is in "raw FADC units' (raus). The simulation convolutes the Compton photon spectrum, shown in Fig. 3(left), with the detector response function determined by the GEANT4 simulation. It includes the non-linearities measured by the 2-LED pulser system. In addition, pile-up effects are incorporated using data taken with a randomly-timed trigger. The simulated Compton spectrum shape was fit to the data with two adjustable parameters, the horizontal scale (to convert to raw FADC units) and vertical scale (counts). The discrepancy observed at the lowest Compton energies (below 2000 raus) is an artifact of the hardware trigger threshold used for this data channel which does not affect the analysis of the threshold-less integrating FADC data used for the primary polarization analyses. These data can also be used for an alternative polarization analysis by constructing histograms of the Compton triggered data sorted by beam-helicity and initial-state photon polarization. These histograms can then be combined to obtain the asymmetries as a function of photon energy. Since the horizontal scale of these data has already been fixed by the fit shown in Fig.5(a), the predicted asymmetry shape can be fit using a single parameter corresponding to the product $P_e P_\gamma$. The results for the two laser polarization states are shown in Fig.5(b) and Fig. 5(c). This approach is accurate to perhaps 2% or so; higher precision requires analysis of the integrated data to avoid uncertainties due to pileup and deadtime effects.

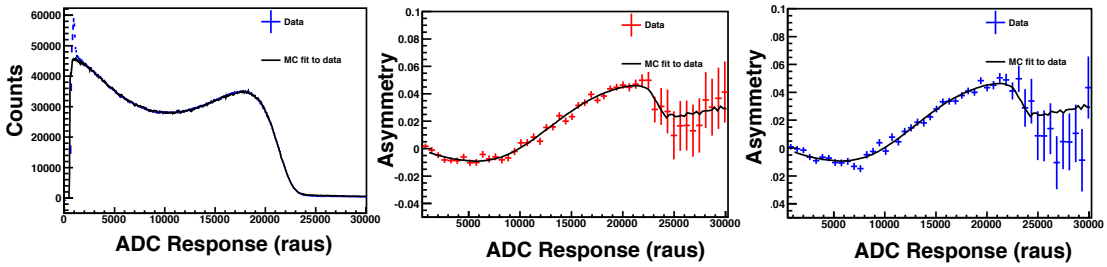

a) Compton Photon Energy Spectrum

b) Asymmetry for Right Circularly-Polarized Photons

c) Asymmetry for Left Circularly-Polarized Photons

Figure 5: The triggered events as a function of calorimeter signal. Panel **a** shows the counts vs photon energy summed over both helicity bins overlaid with the GEANT-based Compton spectrum simulation (solid line). The helicity-dependent asymmetries for the the two photon polarizations are shown in panels **b** and **c**. The fitted asymmetry functions are shown as solid lines.

The upgraded Hall A polarimeter achieved its design goal of 1% during the running of the HAPPEX-III experiment.[7] As shown in Table 1, uncertainty in the polarization of the photons inside the Fabry-Perot cavity was the largest contributor to the total estimated error. We expect that this will be significantly reduced in future running (see talk by D. Jones, this conference). The uncertainty in the signal-weighted analyzing power, A_{IS}, was 0.33% with the largest contribution being due to the limitations of the non-linearity corrections. Uncertainty in the JLab beam energy also contributes since the analyzing power is a function of the electron beam energy. The subtraction of the non-Compton background, measured during the cavity-off cycles, introduces a 0.37% error due to possible shifts of the signal gain and FADC pedestal between the cavity-on and cavity-off measurements. It is worth noting that the non-Compton background is dominated by synchrotron radiation generated by the electron beam as it exits the second dipole and as it enters

Photon Polarization		0.80%
Non-linearity	0.30%	
Energy Uncertainty	0.10%	
Collimator Position	0.05%	
Total Analyzing Power Uncertainty		0.33%
Background Uncertainty	0.31%	
Pedestal Gain Shift	0.20%	
Total Gain Shift Uncertainty		0.37%
Total Uncertainty		**0.94%**

Table 1: Contributions to the Compton beam polarization measurement estimated error for the HAPPEX-III experiment.[5]

the third dipole (see Fig. 2). Since the synchrotron radiation increases as E^4_{beam} for a fixed bending radius, this background would be expected to swamp the Compton signal in JLab's 12 GeV era if no steps are taken to reduce this background. However, Benesch *et al.*[8] have shown that the synchrotron radiation background can be reduced several orders of magnitude by appropriate modification of the chicane magnets fields. These changes have already been implemented in the Hall A Compton chicane.

In summary, the Hall A Compton polarimeter allows continual monitoring of the electron beam's longitudinal polarization. For typical running conditions, the polarization can be determined to 1%. In the near future, reduction of the synchrotron background and improvements in the method used to determine the initial-state photon polarization are expected to reduce the combined systematic error to better than 0.5%. A new microstrip detector will allow a second analysis channel and provide an additional tool for minimizing systematics.

References

[1] A. Denner and S. Dittmaier, Nucl. Phys. B **540**, 58 (1999).

[2] D.S. Parno, Measurements of the Double-Spin Asymmetry A^1 on Helium-3. Toward a Precise Measurement of the Neutron A_1, Ph.D. thesis, Carnegie Mellon University, (2011).

[3] D.S. Parno *et al.*, Nucl. Inst. & Meth. In Phys. Res. A **728**, 92-96 (2013).

[4] M. Friend, A Precision Measurement of the Proton Strange-Quark Form Factors at Q^2 = 0:624 GeV^2, Ph.D. thesis, Carnegie Mellon University, (2012).

[5] M. Friend, *et al.*, Nucl. Inst. & Meth. In Phys. Res. A **676**, 96-105 (2012).

[6] M. Friend, G.B. Franklin, B. Quinn, Nucl. Inst. & Meth. In Phys. Res. A **676**, 66-69 (2012).

[7] Z. Amed *et al.*, Phys. Rev. Lett. **108**, 102001 (2012).

[8] Benesch, *et al.* in preparation.